Single-particle tracking uncovers dynamics of glutamate-induced retrograde transport of NF-κB p65 in living neurons

Article

Accepted Version

Widera, D. ORCID: https://orcid.org/0000-0003-1686-130X, Klenke, C., Nair, D., Heidbreder, M., Malkusch, S., Sibarita, J.-B., Choquet, D., Kaltschmidt, B., Heilemann, M. and Kaltschmidt, C. (2016) Single-particle tracking uncovers dynamics of glutamate-induced retrograde transport of NF-κB p65 in living neurons. Neurophotonics, 3 (4). 041804. ISSN 2329-4248 doi: https://doi.org/10.1117/1.NPh.3.4.041804 Available at https://centaur.reading.ac.uk/63751/

Single-Particle Tracking Uncovers Dynamics of Glutamate-Induced Retrograde Transport of NF-κB p65 in Living Neurons

Darius Widera[1,2,*,#], Christin Klenke[1,*], Deepak Nair[3,4], Meike Heidbreder[5,6], Sebastian Malkusch[9], Jean-Baptiste Sibarita[3,4,7], Daniel Choquet[3,4], Barbara Kaltschmidt,[8,1] Mike Heilemann[9,#] and Christian Kaltschmidt[1,#]

*equal contribution

[1]Cell Biology, University of Bielefeld, Bielefeld, Germany
[2]School of Pharmacy, University of Reading, Reading, United Kingdom
[3]University of Bordeaux, Interdisciplinary Institute for Neuroscience, Bordeaux, France
[4]CNRS UMR 5297, Bordeaux, France
[5]Department of Biotechnology & Biophysics, Julius-Maximilians-Universität, Würzburg, Germany
[6]present address: NSF Erdmann Analytics, Rheda-Wiedenbrück, Germany
[7]Bordeaux Imaging Center, UMS 3420 CNRS, US4 INSERM, University of Bordeaux, France
[8]Molecular Neurobiology, University of Bielefeld, Bielefeld, Germany
[9]Institute for Physical and Theoretical Chemistry, Johann Wolfgang Goethe-University, Frankfurt, Germany

[#]corresponding authors:

Dr Darius Widera
School of Pharmacy, University of Reading
Hopkins Building, Reading, RG6 6AP, United Kingdom
E-mail: d.widera@reading.ac.uk

Prof. Dr. Christian Kaltschmidt
Cell Biology, University of Bielefeld, Universitätsstr. 25,
33501 Bielefeld, Germany
E-mail: c.kaltschmidt@uni-bielefeld.de

Prof. Dr. Mike Heilemann
Institute for Physical and Theoretical Chemistry
Goethe-University Frankfurt
Max-von-Laue-Str. 7
60438 Frankfurt, Germany
E-mail: heilemann@chemie.uni-frankfurt.de

Abstract

Retrograde transport of NF-κB from the synapse to the nucleus in neurons is mediated by the dynein/dynactin motor complex and can be triggered by synaptic activation. The calibre of axons is highly variable ranging down to 100 nm, aggravating the investigation of transport processes in neurites of living neurons using conventional light microscopy. In this study we quantified for the first time the transport of the NF-κB subunit p65 using high-density single-particle tracking in combination with photoactivatable fluorescent proteins in living mouse hippocampal neurons. We detected an increase of the mean diffusion coefficient (D_{mean}) in neurites from 0.12 ± 0.05 $\mu m^2/s$ to 0.61 ± 0.03 $\mu m^2/s$ after stimulation with glutamate. We further observed that the relative amount of retrogradely transported p65 molecules is increased after stimulation. Glutamate treatment resulted in an increase of the mean retrograde velocity from 10.9 ± 1.9 to 15 ± 4.9 μm/s, whereas a velocity increase from 9 ± 1.3 to 14 ± 3 μm/s was observed for anterogradely transported p65. This study demonstrates for the first time that glutamate stimulation leads to an increased mobility of single NF-κB p65 molecules in neurites of living hippocampal neurons.

Keywords: retrograde transport, SPT-PALM; single molecule; NF-kappaB; neurons

Introduction

The inducible transcription factor NF-κB is involved in crucial brain functions including learning and memory formation (1-7). The most abundant NF-κB heterodimer detected within the central nervous system (CNS) is composed of p65 and p50 (3, 8, 9). We and others have shown that NF-κB is localized in the synapse, can be activated by glutamate at synaptic sites, and is transported back to the nucleus after its activation (3, 10-15).

Axons and dendrites represent specialised neuronal cytoplasmic extensions, where movement by random diffusion alone would not permit efficient and directed delivery of proteins over long distances (16, 17). However, signals generated at synapses must be transported back to the nucleus to regulate gene expression (reviewed in (17)).

Anterograde (away from nucleus) and retrograde (towards the nucleus) transport are crucial for the physiological function of neurons and are mediated by motor proteins including dynein and kinesins (18, 19). Due to their polarised nature and the relatively long distance between the nucleus and the periphery, neurons are highly dependent on intact active transport machinery (reviewed in (20)). Consequently, defects in axonal transport are involved in development of several neurodegenerative diseases, including Alzheimer's, Parkinson`s, and Huntington`s disease (21). We and others have previously demonstrated neuronal NF-κB is actively transported towards the nucleus by the minus end-directed motor protein dynein ((11, 22, 23), Fig. 1). In contrast, diffusion seems to be sufficient for its retrograde transport in non-neuronal cells (24). However, the exact biophysical parameters such as diffusion coefficients and velocity of retrogradely transported NF-κB were unknown.

Single-particle tracking (SPT) of fluorophore-labelled receptors in the plasma membrane of a live cell provides valuable information on dynamics and interactions (25). In combination with photoswitchable fluorophores (26), SPT allows the observation a large number of molecules by stochastically activating only a small subset of fluorophores at a given time and tracking them until photobleaching. This cycle of photoactivation, tracking and photobleaching is repeated many (often a few thousand) times. Profiting from the pool of labelled biomolecules in a sample, a large number of single-molecule trajectories are recorded. Single-particle tracking with photoactivated-localization microscopy (SPT-PALM, (27)) allows longer observation times, provides better statistics (28, 29) and allows high-density mapping of molecular movements (30).

In order to study the dynamics of retrogradely transported NF-κB in neurons at the single-molecule level, we applied SPT-PALM (27, 31) and used the fluorescent protein tandem-Eos-FP (tdEos) as a reporter (27, 28). tdEos is photoconverted from a green-fluorescent to an orange-fluorescent species by irradiation with 405 nm light (32). Following this procedure, a small stochastic subset of the tdEos is transferred into the active (orange-fluorescent) state and tracked as single molecules. In the present study, we used this technique to visualise p65-tdEos (NF-κB subunit fused to tdEos) with a localization precision of 26 nm (Fig. 2A).

We investigated the glutamate-induced transport of NF-κB p65 in living hippocampal neurons with single-molecule resolution and determined the respective diffusion coefficients. Finally, we demonstrated that synaptic activity leads to an increased mobility of retrogradely and anterogradely transported neuronal NF-κB p65.

Results and Discussion

Hippocampal neurons transfected with p65-tdEos were identified by widefield imaging detecting the green fluorescence signal from unconverted p65-tdEos. After identification of the soma (containing the nucleus), neurites of transfected cells were irradiated with low intensities of UV light and single p65-tdEos molecules were tracked by their orange

fluorescence. Several thousands of trajectories per cell were recorded and used to generate a trajectory map (Fig. 2B).

Next, we compared the mobility of NF-κB p65 in unstimulated and glutamate-treated neurons. We observed that glutamate treatment led to an increased mobility of p65-tdEos particles compared to the baseline control (Fig. 2B). This increase in mobility is in general accordance with the reports on rapid retrograde transport of NF-κB in neurons after glutamate treatment (11, 22).

We then calculated the mean diffusion coefficient (D_{mean}) of p65-tdEos molecules from the SPT-PALM data (Fig. 3). In the absence of stimulation (baseline) p65-tdEos molecules showed a D_{mean} of 0.12 ± 0.05 $\mu m^2/s$ (Fig. 3A). Stimulation with glutamate resulted in a higher occurrence of fast molecules (D_{mean} of 0.61 ± 0.03 $\mu m^2/s$) compared to unstimulated controls (Fig. 3A-B) and narrowed the distribution of single-molecule diffusion coefficients (Fig. 3A-B). Notably, the D_{mean} measured for p65-tdEos without stimulation is in a similar range than diffusion coefficient reported for the cytoplasmic HIV Gag-Eos fusion (0.11 ± 0.08 $\mu m^2/s$) (27). After stimulation with glutamate, D_{mean} of p65-tdEos is similar to mobile fraction of membrane residing α-amino-3-hydroxy-5-methyl-4-isoxazolepropionic acid (AMPA) receptors with a diffusion coefficient of >0.5 $\mu m^2/s$ (33). We further followed how the mobility of p65-tdEos developed with time and found that the glutamate-dependent increase in D_{mean} persists for at least 400 s (Fig. 3D).

Next, we determined the extent to which glutamate affects the immobile fraction as well as retrogradely and anterogradely transported p65-tdEos particles. In glutamate-stimulated neurons, we recorded a lower occurrence of immobile molecules in neurites that was accompanied by significant increase in retrogradely transported p65-tdEos (Fig. 4A). Further, although not significant, a slight increase of anterogradely transported molecules was measured. Finally, we determined the velocities of single transported p65-tdEos particles. Although glutamate treatment resulted in heterogeneous velocity distribution for both retrograde and anterograde transport, a significantly increased mean velocity was assessed

in both directions (Fig. 4B). Specifically, glutamate treatment resulted in an increase of the mean retrograde velocity from 10.9 ± 1.9 to 15 ± 4.9 µm/s, whereas a mean velocity increase from 9 ± 1.3 to 14 ± 3 µm/s was observed for the anterograde transport. Notably, the mean velocities calculated for p65-tdEos are in the same range reported for the transport of NGF in neurites of rat sympathetic neurons (~3-6 µm/s) as measured in compartmented cultures after applying radioactive ^{125}I-NGF (34). In neuronal cells, the transport of mitochondria is accomplished by microtubule-based motors (kinesins and dynein) with velocities ranging from ~5-30 µm/s (35). Moreover, flagellar dyneins achieve a velocity of up to 19 µm/s (reviewed in (36) and (37)), which is again in general accordance with the mean velocity of 15 µm/s for p65-tdEos after glutamate treatment (this study).

In summary, we report that glutamate stimulation promotes an increase in mobility of the NF-kB subunit p65 in living hippocampal neurons. Exposure of neurons to glutamate leads to an increased mean diffusion coefficient of p65-tdEos and an increase in the velocity of both-retrogradely and anterogradely transported NF-κB p65 in neurites.

Methods

Astrocyte cultures

Mouse astrocytes were prepared from the cortex of postnatal day 1 (P1) BL6 mice, after treatment with 1x Trypsin/EDTA (PAA, Pasching, Austria). The astrocytes were washed with pre-warmed DMEM (37°C, PAA) and transferred to DMEM containing 2 mM L-glutamine, 100 U/ml penicillin and streptomycin and 10 % fetal bovine serum (PAA). Cells were cultured in a humidified incubator at 95% air, 5% CO_2. 1 day prior to hippocampi preparation, astrocyte growth was blocked with 10 µg/ml mitomycin (Sigma-Aldrich, Deisenhofen, Germany) for 1.5 h followed by washing with DMEM (PAA) and cultivation in DMEM supplemented with 2mM L-glutamine, 100U/ml penicillin and streptomycin and 10% fetal

bovine serum (PAA). Prior to preparation of the hippocampi, the astrocytes were transferred to pre-warmed Neurobasal medium (Invitrogen, Darmstadt, Germany) containing B27 supplement (Invitrogen), 2 mM L-glutamine (PAA), 100 U/ml penicillin (PAA) and 100 U/ml streptomycin (PAA).

Hippocampal neuron cultures

Primary cultures of mouse hippocampal neurons were prepared from the hippocampi of E18-E19 BL6 mouse embryos, after treatment with 1x Trypsin/ETDA (15 min, 37°C; (0.05 % / 0.002 % in PBS), PAA). The hippocampi were washed with pre-warmed DMEM (37° C) containing 10 % FCS, to stop trypsin activity and transferred to pre-warmed DMEM (PAA) supplemented with 2 mM L-glutamine, 100 U/ml penicillin (PAA) and 100 U/ml streptomycin (PAA) and 10 % foetal bovine serum (PAA). The cells were dissociated under these conditions using a fire-polished Pasteur pipette followed by seeding on poly-D-Lysine (Sigma-Aldrich) coated coverslips at a density of 50,000 cells/18 mm. The cultures were maintained in a humidified incubator at 5 % CO_2 for 60 min to allow adherence. Subsequently, neurons on coverslips were placed on top astrocyte cultures and further cultivated at 5 % CO_2.

Anaesthesia of neuronal activity for baseline of nuclear NF-κB and glutamate treatment

24 h prior to experimentation, hippocampal neuron cultures were treated with 40 µM 6-cyano-7-nitroquinoxaline-2,3-dione (CNQX, Sigma-Aldrich), 100 µM 2-amino-5-phosphonopentanoic acid (APV, Sigma-Aldrich) and 10 µM nimodipine (Sigma-Aldrich) to establish a stable and low baseline of nuclear NF-κB as described before (22, 23). Afterwards, neurons were washed and exposed to 300 µM glutamate or PBS (Sigma-Aldrich) for 5 min in the absence of the inhibitors at 37°C. Subsequently, the stimulus was washed out and cultures were incubated with complete medium at 37°C for 90 min.

Immunocytochemical staining

Immunocytochemistry was performed as described in (22). Briefly, neurons were fixed in 3.7% PFA for 60 min at 4°C, permeabilised with 0.1% Triton X-100 in PBS followed by incubation with rabbit polyclonal anti- NF-κB p65 antibody (sc-109; Santa Cruz Biotechnology, Inc., Santa Cruz, CA) diluted 1:100. Neurons were washed and incubated with goat anti-rabbit antibody coupled to Cy3 (1:300, Jackson Immuno Research Laboratories, distributed by Dianova, Hamburg, Germany). Nuclear staining was performed with SYTOX (1:10000, Molecular Probes, Göttingen, Germany).

SPT-PALM imaging, single molecule segmentation and tracking

The tdEos fusion to p65 was achieved by subcloning of p65 (38) into pcDNA3-Flag1-td-EosFP (MoBiTec). Hippocampal neurons were transiently transfected with p65-tdEos overnight using Effectene (Qiagen) according to the manufacturer's guidelines. Cells were imaged at 37°C in an open chamber (Ludin Chamber, Life Imaging Services) mounted on an inverted motorized microscope (Nikon Ti-E, Nikon, Japan) equipped with a 100x1.45NA PL-APO (Nikon) objective and a perfect focus system. To identify transfected cells, the fluorescence from the non-photoconverted tdEos was recorded using excitation light at 488 nm and a GFP filter cube (ET470/40, T495LPXR, ET525/50, Chroma, USA). Cells expressing the tdEos constructs were selected for SPT-PALM imaging. Irradiation at 405 nm using a diode laser (Omicron, USA) at low intensities lead to photoconversion of tdEos which was read-out with a 561 nm laser (Cobolt, Sweden). The respective irradiation intensities were adjusted to keep the number of the stochastically activated molecules at low single molecule density, and leave single molecules fluorescent during multiple frames before bleaching. The fluorescence was collected by the combination of a dichroic and emission filters (D101-R561 and F39-617 respectively, Chroma, USA) and a sensitive EMCCD camera (Evolve, Photometric, USA). The acquisition was steered by Metamorph software (Molecular Devices) in streaming mode at 50 frames per second (20 ms exposure time). Recording times for single cells varied from 5 min to 30 min. Single molecule fluorescent spots were

localized in each image frame and tracked over time using a combination of wavelet segmentation and simulated annealing algorithms (39-41). The localization accuracy of the SPT-PALM microscope under our experimental conditions was quantified by using fixed samples expressing tdEos. Localization precision was determined to 26 nm using a nearest neighbour approach, according to (42). The software package used to visualize and derive quantitative data on protein localization and dynamics was custom written for Metamorph (Visitron Systems GmbH, Puchheim, Germany).

An average of > 500 trajectories per cell with a minimum trajectory length of 8 frames was obtained and analysed. For these trajectories, the mean square displacement (MSD) was calculated according to the formula $MSD = \Delta x^2 + \Delta y^2$. The diffusion coefficient was extracted by approximating the first 4 points of a plot of D_{mean} versus time using the relationship of $MSD = 4\mathrm{Dt}$. The mean diffusion coefficient (D_{mean}) was calculated as an average from all single-molecule diffusion. Kymographs were used to define immobile, retrogradely and anterogradely moving particles (according to the position of the soma and the neurites). For exemplary MSD-analysis see Fig. 2C.

Statistical analysis

Statistical significance was determined by ANOVA using Bonferroni post-test, or if appropriate using two-tailed Student's t-tests using GraphPad`s Prim Software. P values < 0.05 were considered significant.

Competing interests

The authors declare that they have no competing interests.

Acknowledgements

This study was supported by the grant of the German research foundation (DFG) to CK. MeH, MiH and SM were supported by the Systems Biology Initiative (FORSYS, grant 0135262) of the German Ministry of Research and Education (BMBF) and the German

research foundation (SFB 902). DN was supported by a Marie-Curie Intra European Fellowship. The authors declare no competing financial interests. We thank Dr Graeme Cottrell for critical reading.

Figure legends

Figure 1. Synaptic activity promotes dynein-dependent retrograde transport of NF-κB to the nucleus. A. Hippocampal neurons were treated with 300 µM glutamate for 5 min. Cells were fixed (90 min after glutamate exposure) and visualised by SYTOX nuclear staining (green) and anti NF-κB p65 immunofluorescence (magenta) to monitor neuronal transport of NF-κB (data from (22), CC BY license). Note that glutamate promotes nuclear translocation of NF-κB subunit p65. **B.** Schematic presentation of retrograde transport of NF-κB in neurons. After stimulation of the neuron with an activator such as glutamate, upstream kinases induce phosphorylation of the inhibitory protein IκB stimulating its proteasomal degradation. This allows the binding of p65/p50 heterodimers to the dynein/dynactin motor proteins. After the assembly of the complex and its retrograde movement along the microtubule network, NF-κB translocates into the nucleus without disruption of the complex and induces transcription of specific target genes.

Figure 2. SPT-PALM imaging of NF-κB p65 in hippocampal neurons. A. The NF-κB p65 subunit was fused to the photoactivatable fluorescent protein tandem-Eos-FP (tdEos) that can be photoconverted by irradiation with UV light. Transfected neurons were identified in widefield fluorescence mode by detecting the green fluorescence signal of the tdEos in p65-tdEos. A small stochastic subset of the p65-tdEos was photoconverted from a green-fluorescent to an orange-fluorescent species and tracked as single molecules. Localization precision for tdEos was determined to 26 nm using a nearest neighbour approach, as described in (42). **B.** Map of single particle trajectories (middle and lower panel) revealed highly increased mobility of p65-tdEos in neurites after glutamate stimulation compared to controls. Representative data set from a single cell for both conditions is shown. C. **Exemplary MSD plots from single-molecule trajectories of untreated (blue) and**

glutamate-treated (red) p65-tdEos. The first four MSD values were considered for extracting the diffusion coefficient.

Figure. 3. A-B. Effect of glutamate on the distribution of diffusion coefficients of NF-κB in hippocampal neurons. Note that glutamate treatment narrows the distribution of single-molecule diffusion coefficients compared to the control. **C.** Average diffusion coefficient D_{mean} of p65-tdEos under baseline conditions and after treatment with glutamate monitored over time (a representative data set from a single cell each is shown). Glutamate treatment leads to significantly increased D_{mean}. Without stimulation p65 molecules showed D_{mean} of 0.12 ± 0.05 $\mu m^2/s$. Stimulation with glutamate resulted in a strongly increased occurrence of fast particles and D_{mean} of p65 to 0.61 ± 0.03 $\mu m^2/s$. **D.** D_{mean} of p65-tdEos under control conditions and after treatment with glutamate monitored over time (a representative data set from a single cell each is shown). Error bars: SEM

Figure 4. A. Effect of glutamate on velocity of retrogradely and anterogradely transported p65-tdEos particles. Single-molecule data was used to calculate the occurrence of immobile and retro- and anterogradely transported p65. Treatment of hippocampal neurons with glutamate resulted in significantly decreased amount of immobile particles and strongly increased retrograde transport. **B.** Glutamate treatment increases the mean velocity of retrogradely and anterogradely transported p65-tdEos.

References

1. M. P. Mattson et al., "Roles of nuclear factor kappaB in neuronal survival and plasticity," *J Neurochem* **74**(2), 443-456 (2000).
2. V. Fridmacher et al., "Forebrain-specific neuronal inhibition of nuclear factor-kappaB activity leads to loss of neuroprotection," *J Neurosci* **23**(28), 9403-9408 (2003).
3. M. K. Meffert et al., "NF-kappa B functions in synaptic signaling and behavior," *Nat Neurosci* **6**(10), 1072-1078 (2003).
4. B. Kaltschmidt, D. Widera, and C. Kaltschmidt, "Signaling via NF-kappaB in the nervous system," *Biochimica et biophysica acta* **1745**(3), 287-299 (2005).

5. M. K. Meffert, and D. Baltimore, "Physiological functions for brain NF-kappaB," *Trends Neurosci* **28**(1), 37-43 (2005).

6. M. P. Mattson, and M. K. Meffert, "Roles for NF-kappaB in nerve cell survival, plasticity, and disease," *Cell Death Differ* **13**(5), 852-860 (2006).

7. B. Kaltschmidt, and C. Kaltschmidt, "NF-kappaB in the nervous system," *Cold Spring Harb Perspect Biol* **1**(3), a001271 (2009).

8. C. Kaltschmidt, B. Kaltschmidt, and P. A. Baeuerle, "Brain synapses contain inducible forms of the transcription factor NF-kappa B," *Mechanisms of development* **43**(2-3), 135-147 (1993).

9. C. Kaltschmidt et al., "Constitutive NF-kappa B activity in neurons," *Mol Cell Biol* **14**(6), 3981-3992 (1994).

10. C. Kaltschmidt, B. Kaltschmidt, and P. A. Baeuerle, "Stimulation of ionotropic glutamate receptors activates transcription factor NF-kappa B in primary neurons," *Proc Natl Acad Sci U S A* **92**(21), 9618-9622 (1995).

11. H. Wellmann, B. Kaltschmidt, and C. Kaltschmidt, "Retrograde transport of transcription factor NF-kappa B in living neurons," *J Biol Chem* **276**(15), 11821-11829 (2001).

12. T. Suzuki et al., "Presence of NF-kB-like and IkB-like immunoreactivities in postsynaptic densities," *Neuroreport* **8**(13), 2931-2935 (1997).

13. P. J. Meberg et al., "Gene expression of the transcription factor NF-kB in hippocampus: regulation by synaptic activity," *Mol. Brain Res.* **38**(2), 179-190 (1996).

14. A. Salles, A. Romano, and R. Freudenthal, "Synaptic NF-kappa B pathway in neuronal plasticity and memory," *J Physiol Paris* **108**(4-6), 256-262 (2014).

15. B. Kaltschmidt, and C. Kaltschmidt, "NF-KappaB in Long-Term Memory and Structural Plasticity in the Adult Mammalian Brain," *Front Mol Neurosci* **8**(69 (2015).

16. C. L. Howe, "Modeling the signaling endosome hypothesis: why a drive to the nucleus is better than a (random) walk," *Theor Biol Med Model* **2**(43 (2005).

17. T. H. Ch'ng, and K. C. Martin, "Synapse-to-nucleus signaling," *Curr Opin Neurobiol* **21**(2), 345-352 (2010).

18. S. Hanz, and M. Fainzilber, "Integration of retrograde axonal and nuclear transport mechanisms in neurons: implications for therapeutics," *Neuroscientist* **10**(5), 404-408 (2004).

19. R. B. Vallee et al., "Dynein: An ancient motor protein involved in multiple modes of transport," *J Neurobiol* **58**(2), 189-200 (2004).

20. S. Maday et al., "Axonal transport: cargo-specific mechanisms of motility and regulation," *Neuron* **84**(2), 292-309 (2014).

21. S. Millecamps, and J. P. Julien, "Axonal transport deficits and neurodegenerative diseases," *Nature reviews. Neuroscience* **14**(3), 161-176 (2013).

22. I. Mikenberg et al., "Transcription factor NF-kappaB is transported to the nucleus via cytoplasmic dynein/dynactin motor complex in hippocampal neurons," *PLoS One* **2**(7), e589 (2007).

23. C. K. Shrum, D. Defrancisco, and M. K. Meffert, "Stimulated nuclear translocation of NF-kappaB and shuttling differentially depend on dynein and the dynactin complex," *Proc Natl Acad Sci U S A* **106**(8), 2647-2652 (2009).

24. I. Mikenberg et al., "TNF-alpha mediated transport of NF-kappaB to the nucleus is independent of the cytoskeleton-based transport system in non-neuronal cells," *European journal of cell biology* **85**(6), 529-536 (2006).

25. G. J. Schutz, H. Schindler, and T. Schmidt, "Single-molecule microscopy on model membranes reveals anomalous diffusion," *Biophys J* **73**(2), 1073-1080 (1997).

26. A. Furstenberg, and M. Heilemann, "Single-molecule localization microscopy-near-molecular spatial resolution in light microscopy with photoswitchable fluorophores," *Phys Chem Chem Phys* **15**(36), 14919-14930 (2013).

27. S. Manley et al., "High-density mapping of single-molecule trajectories with photoactivated localization microscopy," *Nature methods* **5**(2), 155-157 (2008).

28. M. Heidbreder et al., "TNF-alpha influences the lateral dynamics of TNF receptor I in living cells," *Biochimica et biophysica acta* **1823**(10), 1984-1989 (2012).

29. P. J. Zessin, A. Sporbert, and M. Heilemann, "PCNA appears in two populations of slow and fast diffusion with a constant ratio throughout S-phase in replicating mammalian cells," *Sci Rep* **6**(18779 (2016).

30. D. Nair et al., "Super-resolution imaging reveals that AMPA receptors inside synapses are dynamically organized in nanodomains regulated by PSD95," *J Neurosci* **33**(32), 13204-13224 (2013).

31. J. B. Sibarita, "High-density single-particle tracking: quantifying molecule organization and dynamics at the nanoscale," *Histochemistry and cell biology* **141**(6), 587-595 (2014).

32. J. Wiedenmann et al., "EosFP, a fluorescent marker protein with UV-inducible green-to-red fluorescence conversion," *Proceedings of the National Academy of Sciences of the United States of America* **101**(45), 15905-15910 (2004).

33. P. Opazo et al., "CaMKII triggers the diffusional trapping of surface AMPARs through phosphorylation of stargazin," *Neuron* **67**(2), 239-252 (2010).

34. D. R. Ure, and R. B. Campenot, "Retrograde transport and steady-state distribution of 125I-nerve growth factor in rat sympathetic neurons in compartmented cultures," *J Neurosci* **17**(4), 1282-1290 (1997).

35. W. Song et al., "Mutant huntingtin binds the mitochondrial fission GTPase dynamin-related protein-1 and increases its enzymatic activity," *Nature medicine* **17**(3), 377-382 (2011).

36. D. D. Ginty, and R. A. Segal, "Retrograde neurotrophin signaling: Trk-ing along the axon," *Curr Opin Neurobiol* **12**(3), 268-274 (2002).

37. R. B. Campenot, and B. L. MacInnis, "Retrograde transport of neurotrophins: fact and function," *J Neurobiol* **58**(2), 217-229 (2004).

38. C. Klenke et al., "Hsc70 is a novel interactor of NF-kappaB p65 in living hippocampal neurons," *PLoS One* **8**(6), e65280 (2013).

39. I. Izeddin et al., "Wavelet analysis for single molecule localization microscopy," *Opt Express* **20**(3), 2081-2095 (2012).

40. V. Racine et al., "Visualization and quantification of vesicle trafficking on a three-dimensional cytoskeleton network in living cells," *J Microsc* **225**(Pt 3), 214-228 (2007).

41. V. Racine et al., "Multiple-target tracking of 3D fluorescent objects based on simulated annealing," *Biomedical Imaging: Nano to Macro, 2006. 3rd IEEE International Symposium on* 1020-1023 (2006).

42. U. Endesfelder et al., "A simple method to estimate the average localization precision of a single-molecule localization microscopy experiment," *Histochemistry and cell biology* **141**(6), 629-638 (2014).

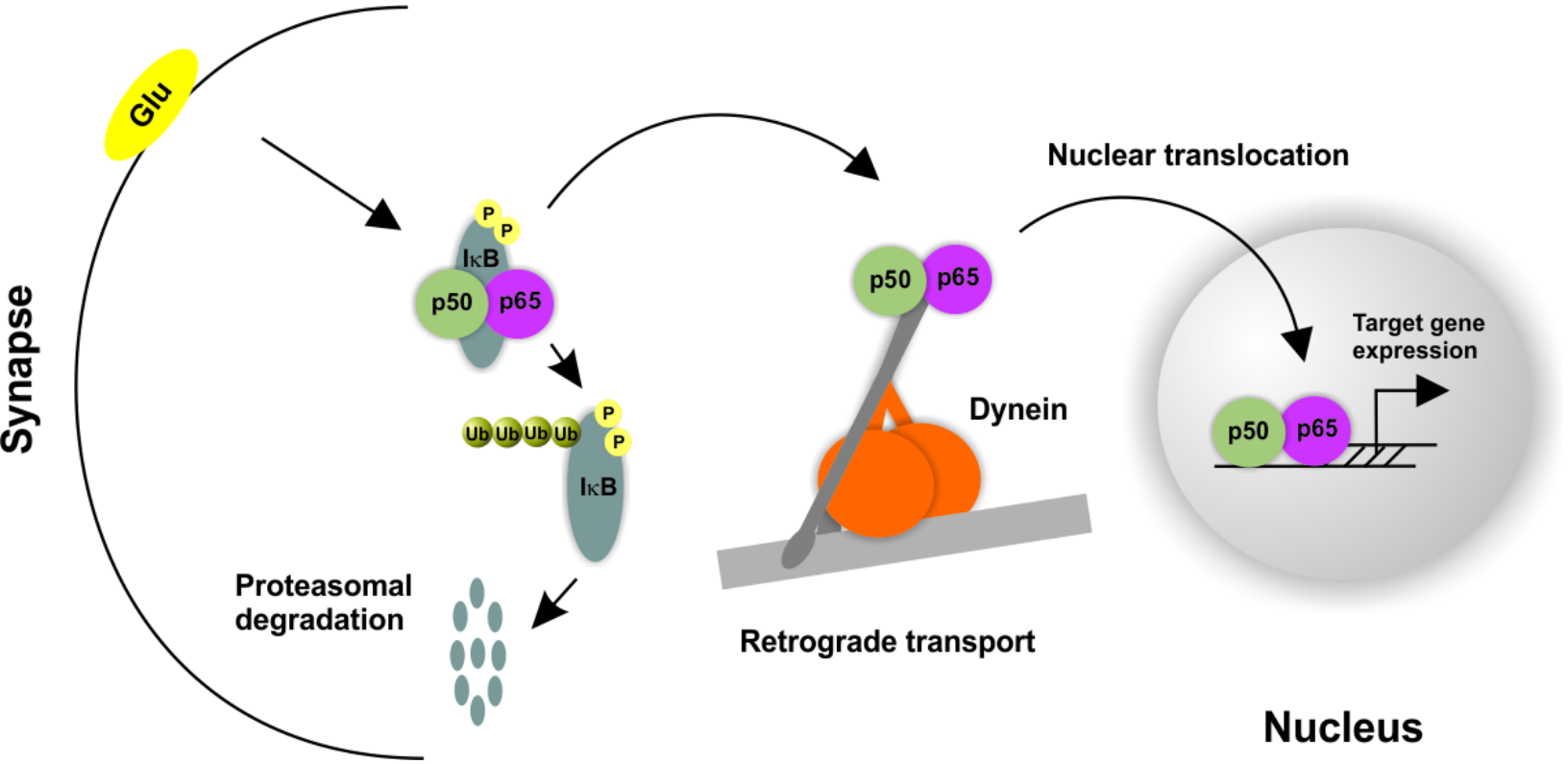
Synapse
Glu
P
P
IκB
p50
p65
Ub
Ub
Ub
Ub
P
P
IκB
Proteasomal
degradation
p50
p65
Dynein
Retrograde transport
Nuclear translocation
Target gene
expression
p50
p65
Nucleus

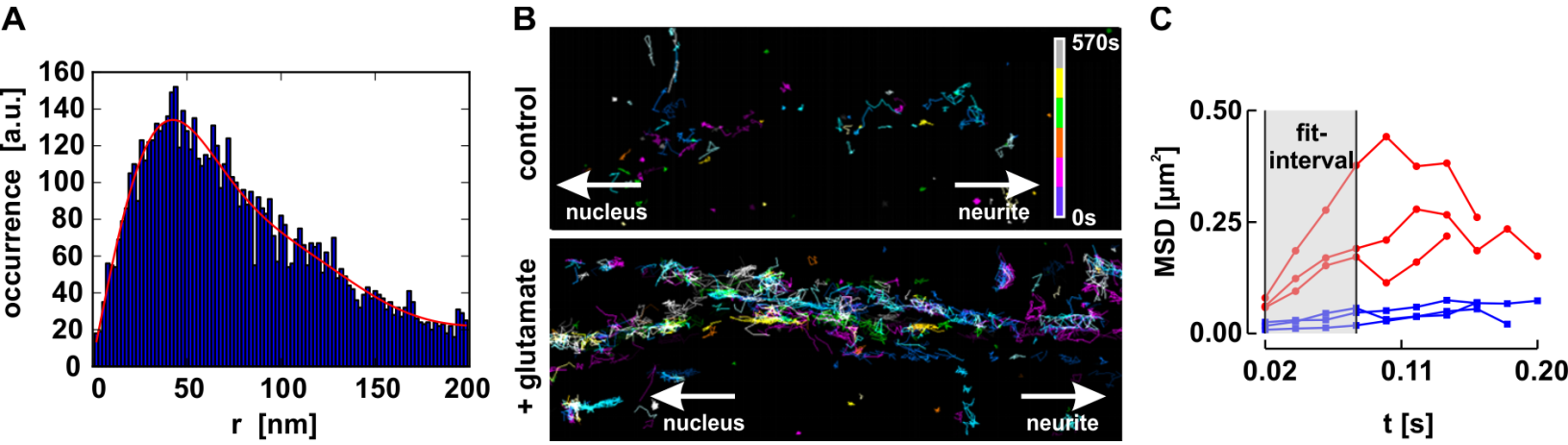
A
occurrence [a.u.]
160
140
120
100
80
60
40
20
0
0
50
100
150
200
r [nm]
B
control
570s
0s
nucleus
neurite
+ glutamate
nucleus
neurite
C
MSD [µm²]
0.50
0.25
0.00
fit-
interval
0.02
0.11
0.20
t [s]

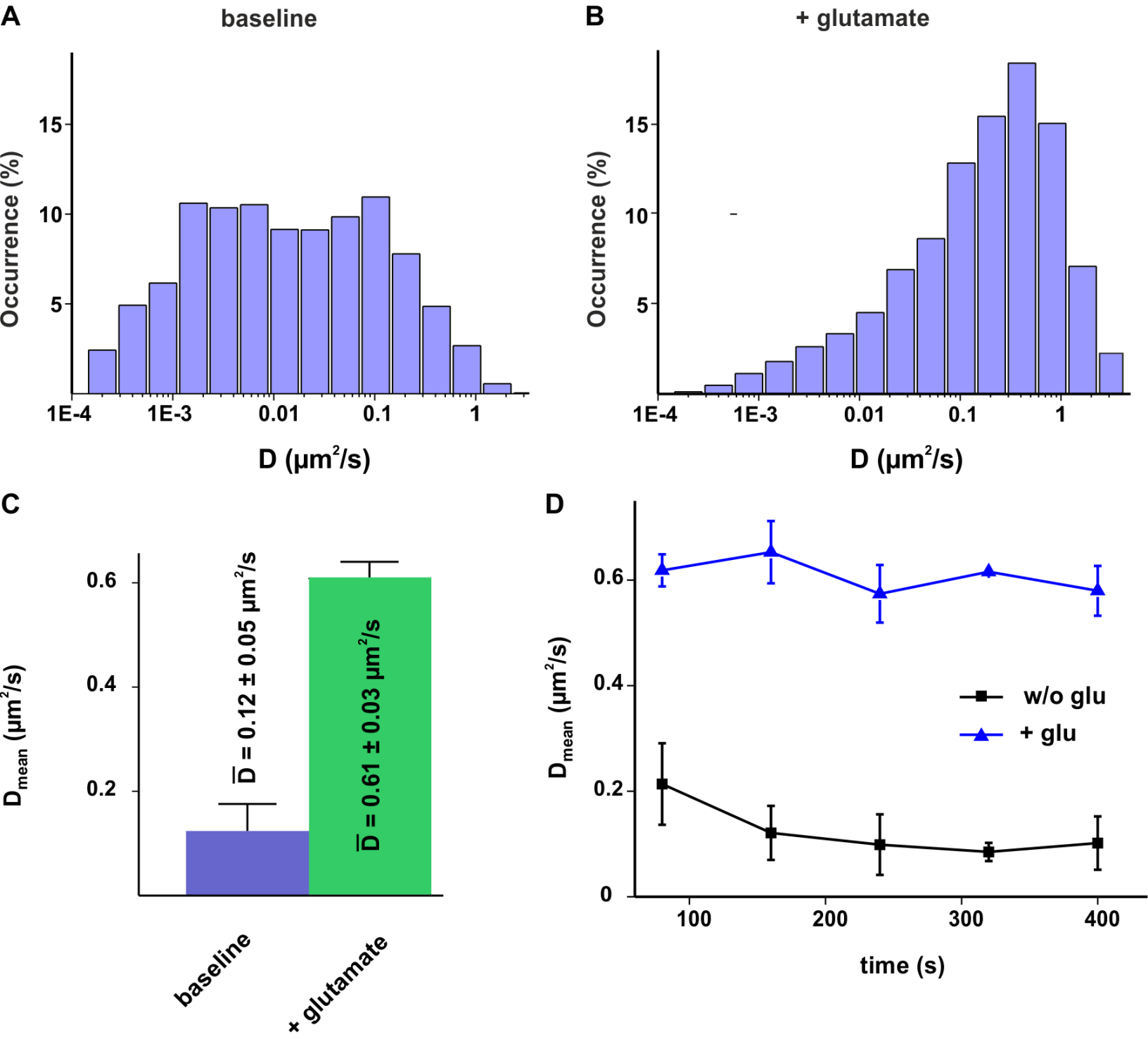
A
baseline
B
+ glutamate
Occurrence (%)
15
10
5
1E-4
1E-3
0.01
0.1
1
D (μm²/s)
C
D
0.6
0.4
0.2
0
D_mean (μm²/s)
D̄ = 0.12 ± 0.05 μm²/s
D̄ = 0.61 ± 0.03 μm²/s
baseline
+ glutamate
w/o glu
+ glu
100
200
300
400
time (s)

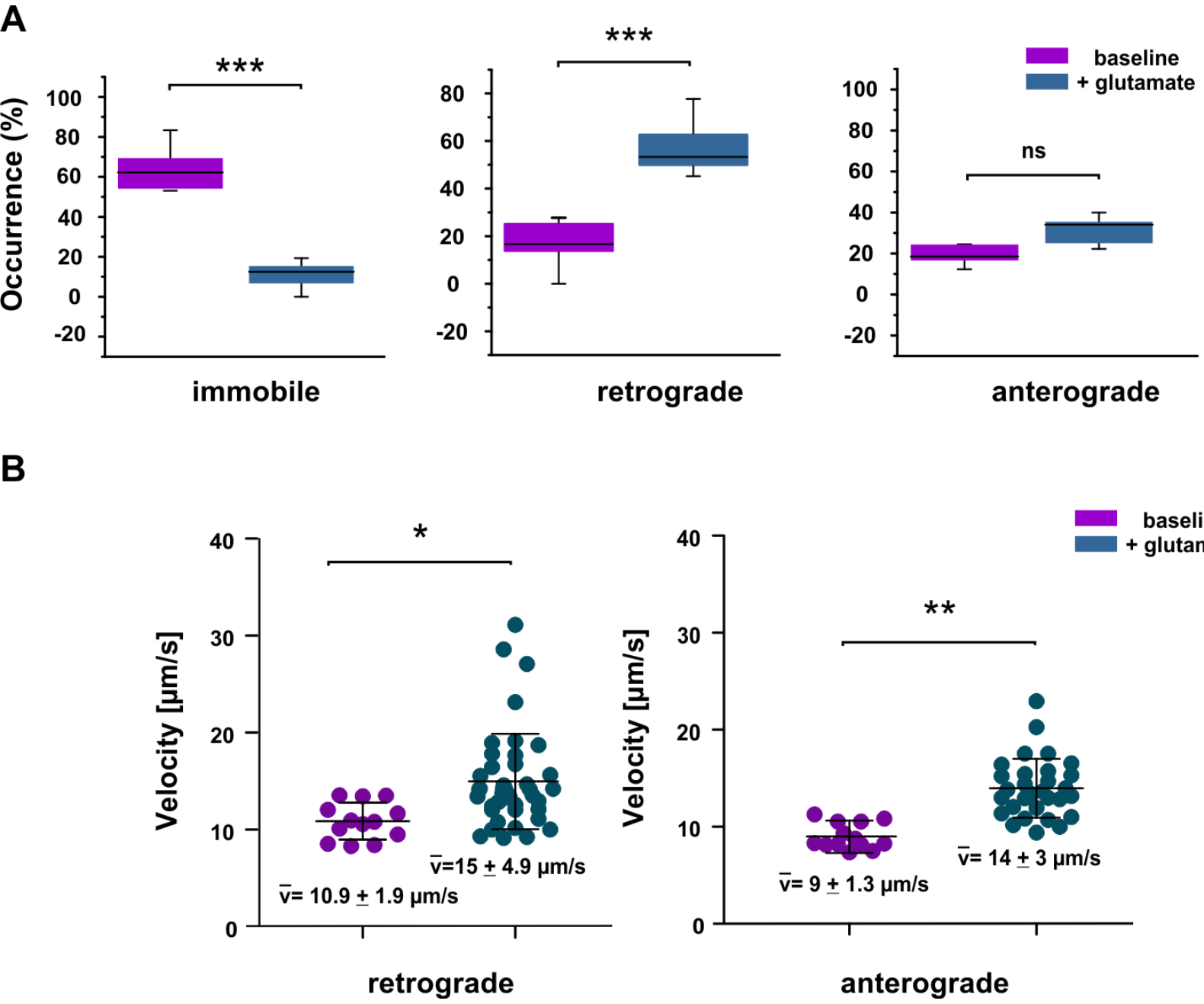
A
***
***
ns
baseline
+ glutamate
Occurrence (%)
100
80
60
40
20
0
-20
immobile
retrograde
anterograde
B
*
**
baseline
+ glutamate
Velocity [µm/s]
40
30
20
10
0
v̄= 10.9 ± 1.9 µm/s
v̄=15 ± 4.9 µm/s
v̄= 9 ± 1.3 µm/s
v̄= 14 ± 3 µm/s
retrograde
anterograde